A NEW 2-D MODEL FOR INHOMOGENEOUS PERMANENT MAGNETS

A. KTENA, D.I. FOTIADIS and C.V. MASSALAS

17-99

Preprint no. 17-99/1999

Department of Computer Science
University of Ioannina
451 10 Ioannina, Greece

A NEW 2-D MODEL FOR INHOMOGENEOUS PERMANENT MAGNETS

A. Ktena[(1)], D.I.Fotiadis[(1)], and C. V. Massalas[(2)]

[(1)] Dept. of Computer Science, University of Ioannina, GR 451 10 Ioannina, Greece

[(2)] Dept. of Mathematics, University of Ioannina, GR 451 10 Ioannina, Greece

Keywords: Inhomogeneous Magnets; 2-D Preisach Model; Nucleation Field.

SUMMARY

Comparison of existing solutions for the nucleation field of one soft spherical inclusion in a hard magnetic matrix is carried out. A new 2-D model for inhomogeneous permanent magnets (RE-TM) is proposed. The new model is based on the Preisach formalism. The intrinsic properties of the material are related to the model parameters. The effect of the latter on the major loop characteristic is shown. The major and minor loop behavior along the easy and hard axes is successfully reproduced

1. INTRODUCTION

The reversal of magnetization in ferromagnetic materials is a non-linear process because of the hysteresis of the magnetization response (output) to the applied magnetic field (input). It involves both irreversible switching and reversible rotation of the magnetization of the particles or grains in the medium. Both processes depend on the intrinsic properties and microstructure of the material, and the complex network of interactions developed.

The models attempting to describe the magnetization reversal are usually based on the micromagnetic approach [1-6]. The starting point is the free energy equation of the magnet, the minimization of which, with respect to the magnetization direction, yields the states of thermomagnetic equilibrium. The solution(s) of the minimized energy equation correspond(s) to the nucleation field of the material, the field at which magnetization reversal starts.

This approach allows for a detailed description of the microstructure of the material and the developing interactions because of the different energy density terms that contribute to the energy equation. However, the resulting equation is also an implicit function of the magnetization direction, which makes the solution of the general form of the energy equation extremely cumbersome. In the quest for such solutions, researchers have either used convenient geometries and microstructures [1-3] in order to obtain analytical expressions for the nucleation fields or they have used finite element methods to obtain the nucleation fields of more complex systems [4,5].

When a magnetic material is assumed to be homogeneous, perfectly aligned and made of single domain particles the magnetizations of which rotate coherently, the expression obtained for the nucleation field, H_n, is the well-known [1]:

$$H_n = \frac{2K_1}{M_s} - N_{eff} M_s$$

where K_1 and M_s are the first anisotropy constant and saturation magnetization of the material, respectively. The second term describes the effect of self-demagnetizing fields where N_{eff} is the demagnetizing factor. This expression is referred to as the

ideal nucleation field because first, the actual coercive fields measured in the laboratory are lower by orders of magnitude and second, no real magnet has a microstructure compatible with the assumptions underlying this expression.

On the other hand, there exist models which consider magnetic materials, or systems exhibiting hysteresis, in general, as black-boxes with known inputs (applied fields) and outputs (bulk magnetization). In the case of magnetic hysteresis, such a systematic approach, based on the Preisach formalism, has been successful both in scalar and vector applications[7]. Preisach-type models can be easily implemented and make efficient tools for media design or cumbersome simulations, as in the case of magnetic recording [8]. They tune-in to the material being modeled through the identification process, usually based on simple bulk measurements of macroscopic material properties. The identification may get more complicated as the complexity of the model increases but, on the other hand, a successful and systematic identification method usually implies a successful model since this is what relates the abstract model assumptions and postulations with reality.

The materials that inspired this work are the *inhomogeneous* permanent magnets of the RE-TM type which exhibit an enhanced energy product and coercivity. The hard phase (RE) contributes the high anisotropy and the soft phase (TM) the high remanence. The coercivity and the energy product are further enhanced when the 3d atoms are exchange-coupled to the RE [9]. From a modeling point of view, 3d-alloys are extremely challenging since not only each phase has different magnetic properties but they also interact with each other.

The existing nucleation models deal with the simplified geometry of one soft spherical inclusion, of diameter D, planted inside a hard matrix (shown on fig. 1). The expressions of the nucleation field obtained are more accurate than the ideal nucleation field and contribute to our knowledge of the underlying physics taking into account the different material parameters of the two phases and the interactions between them. A comparison of these analytical solutions is presented in the first part of this paper in an attempt to understand the challenges faced when modeling inhomogeneous materials.

Our conclusions are incorporated in the design of a 2-D model based on the Preisach formalism *which is not constrained by specific geometries or number of soft inclusions and deals with the two phases in a statistical sense*.

2. NUCLEATION MODELS

The main underlying assumption of the nucleation models presented below is that *nucleation*, as opposed to domain wall pinning, is the governing mechanism of the magnetization reversal. Nucleation starts at the soft spherical inclusion of diameter D planted in a hard magnetic matrix perfectly aligned along the direction of the easy axis. The expressions that follow are all based on the minimization and linearization of the free energy (E) equation:

$$E = \int \{E_{ex}(\mathbf{r}) + E_k(\mathbf{r}) + E_a(\mathbf{r}) + E_m(\mathbf{r})\} d\mathbf{r} \tag{1}$$

where E_{ex} is the exchange energy density, E_k is the anisotropy energy density, E_a is the energy density of interaction with the applied field (Zeeman energy density), and E_m is the self-magnetostatic energy density; all are implicit functions of position $\mathbf{r}$:

$$\begin{aligned} E_{ex}(\mathbf{r}) &= A(\mathbf{r})[\nabla \cdot \mathbf{m}(\mathbf{r})]^2 \\ E_k(\mathbf{r}) &= -\left(K_1(\mathbf{r})(\mathbf{n}(\mathbf{r}) \cdot \mathbf{m}(\mathbf{r}))^2 + K_2(\mathbf{r})(\mathbf{n}(\mathbf{r}) \cdot \mathbf{m}(\mathbf{r}))^4 + \ldots.\right) \\ E_a(\mathbf{r}) &= -\mathbf{m}(\mathbf{r}) \cdot \mathbf{H} \\ E_m(\mathbf{r}) &= -\frac{1}{2}\mathbf{M}(\mathbf{r}) \cdot \mathbf{H}_d(\mathbf{r}) \end{aligned} \tag{2}$$

Skomski and Coey model

For an ideally soft inclusion ($K_s = 0$) of radius r_0, Skomski and Coey [2] obtained the following implicit equation for H_n:

$$\frac{A_s}{A_h}\left[r_0\sqrt{\frac{M_s H_n}{2A_s}}\cot\left(\sqrt{\frac{M_s H_n}{2A_s}}\right) - 1\right] + 1 + r_0\sqrt{\frac{2K_h - M_h H_n}{2A_h}} = 0 \tag{3}$$

where A_s, M_s, K_s, and A_h, M_h, K_h are the material parameters of the soft and the hard phase, respectively.

The model of Kronmüller

According to Kronmüller *et al.*, the general form of the nucleation field is:

$$H_n = \alpha(\Delta K, r_0)\frac{2K_1}{M_s} - N_{eff}M_s \tag{4}$$

where a and N_{eff} are the parameters describing the microstructure of the material. $a(\Delta K, r_0)$ is the factor by which the ideal nucleation field is reduced due to a soft inclusion of anisotropy ΔK and width $2r_0$. N_{eff} takes care of the effect of stray fields. Analytical expressions for the parameter $a(\Delta K, r_0)$ have been obtained for one-, and two- dimensional rotation of the magnetization of the nucleated region, and for both harmonic and quasiharmonic diffusion profiles of anisotropy [1]:

- One-dimensional rotation: *harmonic* case

With z being the easy axis, the exchange stiffness $A(z)$ is assumed to be constant throughout the sample and the diffusion profile of the first anisotropy constant is described by:

$$K_1(z) = K_s + \Delta K\left(1 - e^{-\frac{z^2}{r_0^2}}\right) \tag{5}$$

where K_s is the anisotropy constant at the center of the inhomogeneity and $K_1(\infty) = K_s + \Delta K$ is the anisotropy constant of the 'homogeneous' material.

Then:

$$\alpha = \frac{\delta_B}{\pi r_0} + 1 - \frac{\Delta K}{K_1} \tag{6}$$

where $\delta_B = \pi\sqrt{A \cdot \Delta K}$ corresponds to the Bloch wall width of the material when $K_s << K_1(\infty)$.

- One-dimensional rotation: *quasiharmonic* case

The diffusion profile of the first anisotropy constant is now described by:

$$K_1(z) = K_S + \frac{\Delta K}{ch^2\left(-z^2/r_0^2\right)} \tag{7}$$

and

$$\alpha = 1 - \frac{\Delta K}{K_1}\left(\frac{\delta_B}{2\pi r_0}\right)^2\left[-1+\sqrt{1+\frac{4\Delta K r_0^2}{A}}\right]^2 \qquad (8)$$

- Two-dimensional rotation: *harmonic* case

In the case of two-dimensional rotation the inhomogeneity is again infinite in the y-direction but of length L in the x direction and:

$$a = \frac{\delta_B}{\pi r_0^2} + 1 - \frac{\Delta K}{K_1} + \left(\frac{\delta_B}{L}\right)^2 \qquad (9)$$

- Two-dimensional rotation: *quasiharmonic* case

$$a = 1 - \frac{\Delta K}{K_1}\left(\frac{\delta_B}{2\pi r_0}\right)^2\left[-1+\sqrt{1+\frac{4\Delta K r_0^2}{A}}\right]^2 + \left(\frac{\delta_B}{L}\right)^2 \qquad (10)$$

The solutions for the 2 - D rotation predict higher nucleation fields (higher α) than those obtained in the case of 1 - D rotation because of the term containing the length-parameter, L.

We have calculated the reduced nucleation fields according to expressions 3,6 and 8-10 for a sample of anisotropic $Sm_2Fe_{17}N_3$ as a function of the diameter of the inhomogeneity, $2r_0$. The material parameters used are shown in Table 1 and the results in Figs. 1 and 2.

Table 1: Material Properties

Properties	$Sm_2Fe_{17}N_3$ [1]
$(BH)_{max}$	880 KJ/m^3
$\mu_0 M_s$	1.55 T
K_1	12 MJ/m^3
A	10.7×10^{-12} J/m
δ_B	3×10^{-9} m

[1] as reported by Skomski and Coey in Ref.2;

In Fig. 1, the reduced nucleation field ($H_n/H_{n,ideal}$) according to the Skomski and Coey calculation (eq. 3), is plotted against the reduced inclusion diameter $(2r_0/\delta_B)$ for different ratios $A_s/A_h = 1.0, 1.5, 2.0$. Notice the "plateau" region up to diameters equal to the Bloch-wall width [2]. For inclusions of diameter less than δ_B, the nucleation field is equal to the ideal field because of the exchange interactions. For an inclusion of diameter twice the wall width, the nucleation field decreases down to 40% of the ideal one. Varying the exchange constant of the hard phase while keeping that of the soft phase constant we notice that a higher ratio of A_s/A_h yields slightly higher nucleation fields.

In Fig. 2, eqs. (6) and (8) with $\Delta K = 1.0K_1$ are compared against eq. (3) with $A_s/A_h = 1.0$. The results for 2-D rotation predict higher nucleation fields by 10-15% and are not shown here. The "plateau" region breaks down at diameters smaller than the wall width of the hard phase in the cases of eqs. (6) and (8) eventhough the exchange energy in inhomogeneities of that size should be able to prevent deterioration of the ideal nucleation fiel. In the case of the quasiharmonic anisotropy profile (eq. (8)), 40% of the ideal nucleation fields is lost for diameters up to δ_B. For diameters of inclusions higher than $3\delta_B = 9\text{nm}$, all three solutions predict a decrease in the nucleation field down to approximately 10-15% of the ideal one.

4. THE NEW MODEL

The new model adopts the macroscopic approach based on the Preisach formalism but uses solutions for the nucleation field as building blocks or figures of merit. According to the formalism [7], a magnetic material can be described by a characteristic probability density function $\rho(H_+, H_-)$ where H_+ and H_- are the upper and lower switching fields of elementary square loop operators (Fig.4), $\gamma(H_+, H_-) = \pm 1$. We can think of an elementary loop as the switching characteristic of a specific grain or group of grains with identical behavior. When the elementary loop does not experience any interactions, or the sum of the interactions it experiences is zero, it is centered at $H = 0$ and $H_+ = -H = H_c$ with H_c being not the coercivity of the magnet but the coercivity of the "grain" represented by this elementary loop.

When interactions, H_i, are included, the loop is shifted to the left or to the right according to the direction of the resultant interaction force, thus making it easier or harder to switch. For the case shown in Fig. 4, $H_+ = H_c - H_i$ and $H_- = -H_c + H_i$. A probability density function $\rho(H_+, H_-)$ is then defined over a triangular plane, the *Preisach plane*, bounded by $H_c = 0$, $H_+ = H_{sat}$, and $H_- = H_{sat}$ where H_{sat} is the saturation field. The height of the density function over an elementary area $dH_+ dH_-$ depends on the magnetization of the "grains" ensemble contained in it. Integration over the Preisach plane of the density function convolved with the square loop operator yields the magnetization of the material as a function of the applied field

Starting from positive saturation (all operators are in the +1 state) and decreasing the applied field $H < H_{sat}$, all operators with $H > H_1$, will switch to the negative state. If the field increases up to H_2 the operators with $H_+ < H_2$ will revert to the +1 state. This way, for any sequence of fields, a "boundary" separating regions of negative and positive magnetization is obtained, which serves as the "memory" of the system. For the 1-D case this boundary looks like a staircase consisting of horizontal and vertical segments (Fig.3). The magnetization of the material as a function of the applied field $M(H)$, is then the integral of the characteristic material density over the Preisach plane:

$$M(H) = \iint \rho(H_+, H_-)\gamma(H_+, H_-)dH_+ dH_- \qquad (11)$$

The model is complete as long as the pdf $\rho(H_+, H_-)$ and the switching operator $\gamma(H_+, H_-)$ are determined experimentally or analytically.

In the scalar case, the operator $\gamma(H_+, H_-)$ behaves like a switch, which toggles between the +1 and –1 state of the "unit-magnetization" of the "grain". This assumption conforms to the scalar nature of the model but it prevents the model from predicting the reversible component of $M(H)$, which is due to rotation of the **M**-vector and the bowing of domain boundaries. The total susceptibility of a material, defined as the local slope of an M-H curve, has a reversible and an irreversible component: $x_{tot} = x_{rev} + x_{irr}$ where, $x_{tot} = dM/dH$ and $x_{rev} = \partial M/\partial H\big|_{M_{irr}}$ [15]. Reversible behavior on an M-H loop is observed near saturation points where the

relationship between M and H is practically linear (no hysteresis). Near saturation, the magnetization moments of misaligned grains rotate reversibly tending to align fully with the large applied field. In scalar models, the reversible component of the magnetization can be added on to the irreversible component obtained from the Preisach model [14]. Otherwise, a vector model accounting for rotation as well as switching [8] is needed.

In the vector case, the scalar operator $\gamma(H_+, H_-)$ is replaced by a vector one, $\Gamma(H_+, H_-)$. Such an operator is the coherent rotation Stoner-Wohlfarth model which predicts the orientation of the unit magnetization vector, $\mathbf{m}$, under the effect of a normalized external field, $\mathbf{h}$, for a magnetically isolated ellipsoid of revolution with uniaxial anisotropy:

$$\tan\varphi = \left(h_y / h_x\right)^{2/3} \tag{12}$$

where φ is the angle of $\mathbf{m}$ with the easy axis and h_x, h_y are the components of $\mathbf{h}$ along the easy and hard axis respectively. The boundary on the Preisach plane no longer consists of vertical and horizontal segments only. Rotation makes switching easier and the boundary is curved in such a way as to allow for more switching.

The *identification* of the model for a given system/material is related to the characteristic density $\rho(H_+, H_-)$ which cannot be measured directly. It has been shown that $\rho(H_+, H_-) = \rho(H_c, H_i)$ and $\rho(H_c, H_i) = \rho(H_c)\rho(H_i)$ [14]. In this case, one only needs to obtain expressions for, or measure the distributions of, the grain coercivities and interactions in the material being modeled. The parameters of the probability density functions that are used to model $\rho(H_c)$ and $\rho(H_i)$ are then linked to macroscopic or microscopic material properties.

Since the inhomogeneous permanent magnets are RE-TM alloys consisting of a hard and a soft magnetic phase interacting with each other, the new model, in the spirit of the Preisach formalism, takes into account the different characteristics of the two phases. The density of coercive fields $\rho(H_c)$ is the weighed sum of two densities ρ_1 and ρ_2, for the soft and hard phase respectively, with ρ_1 centered at a lower field than

ρ_2. The weight attached to each function depends on the % content of the soft phase, w. The characteristic density (Fig. 4) is then:

$$\rho(H_+, H_-) = \rho(H_c, H_i) = \rho(H_c)\rho(H_i) = \left[w\rho_1(H_{soft}) + (1-w)\rho_2(H_{hard})\right]\rho_3(H_i)$$

The angular dispersion of easy axes is accounted for by the superposition of the response of Preisach planes dispersed around the easy axis according to a fourth distribution $\rho_4(a)$ with a being the angle a plane forms with the easy axis.

For an appropriate switching mechanism, $\Gamma(H_+, H_-)$, the magnetization response of the magnet to a sequence of applied fields ($H_t, t = 0,1,2,....$ is given by:

$$M(H_t) = \int_{-\pi/2}^{\pi/2} \int_{-H_{sat}}^{H_{sat}} \int_{H_i}^{H_{sat}} \rho_4(a)\rho_3(H_i)\left[w\rho_1(H_{c,soft}) + (1-w)\rho(H_{c,hard})\right]\gamma(H_+, H_-)dH_+ dH_- da$$

To identify the model, we need to relate the parameters of ρ_j, with $j = 1,2,3,4$, to macroscopic and, if possibly, microscopic properties of the material, such as the grain size distribution, the coercivity H_c, the exchange constant A, the first anisotropy constant K_1, the saturation magnetization M_s, and the percentage content of each phase as well as the squareness, S, and coercivity squareness, S^*, of the alloy.

5. RESULTS

In order to test the model, we assumed that all the probability density functions ρ_j are Gaussians $N(\mu, \sigma^2)$ of the form:

$$\rho_j(H) = \frac{1}{\sqrt{2\pi\sigma_j^2}} \exp\left[-\frac{(H-\mu_j)^2}{2\sigma_j^2}\right]$$

Fig. 5 shows the major loop and first- and second- order minor loops obtained for the characteristic density of Fig. 4. In Fig. 6, the major loop field sequence is applied along the hard axis. The model exhibits the expected hysteresis behavior in both major and minor loops and has good vector properties. Notice that switching (Fig. 5) begins at fields above $0.6H_c$ while $H_{sat} > 10H_c$ (not shown).

The next step is to study the effect of the densities' parameters on the properties of the M-H curve and investigate their relationship to the material properties.

- The angular dispersion function $\rho_4(a)$ is centered at zero degrees (μ_4=0) to the easy axis with the standard deviation, σ_4, varied between 5° and 25°. This parameter is the *only one* controlling the loop squareness, S, while it affects the coercivity, H_c, as well (Fig 6). Table 2 shows the effect of σ_4, while all other parameters are kept constant, on S and H_c for a number of parameter sets.

Table 2: The effect of σ_4 on H_c and S.

σ_4 (degs)	5	10	15	20	25
S	.997	0.985	0.967	0.949	0.935
H_c (Oe)	2700	2200	2000	1850	1800

- The interactions function $\rho_3(H_i)$ is also centered at zero field on the assumption that the *average* interaction field experienced by the materials is zero. The standard deviation, σ_3, is varied (Fig.7) affecting mainly the slope of the major loop around the coercivity, i.e., the wider the interactions distribution gets, the lower the slope. This behavior suggests a way to distinguish between exchange and magnetostatic interactions since strong exchange interactions result in loops with high S^* and a narrow interactions distribution does the same thing in the model. This parameter is also related to the grain size since larger grains favor magnetostatic interactions and smaller ones are exchange coupled.

- The soft and the hard phase coercivity functions, $\rho_1(H_{c,soft})$ and $\rho_2(H_{c,hard})$, are centered at their respective ideal nucleation fields:

$$\mu_j = \frac{2K_{1,j}}{M_{s,j}}$$

where $j=1$ for the soft phase and $j=2$ for the hard phase. The coercivity of the M-H curve depends on the mean values ($\mu_1 < H_c < \mu_2$) of the two distributions as well as on their standard deviations (σ_1 and σ_2). The coercivity of the magnet is

affected by the grain size as well. Larger grains lead to a logarithmic decrease of H_c since stray fields become of importance at negative applied fields [16]. The grain size effect has not been included at this stage.

- Finally the % content (w) of the soft phase was varied from 1 to 60%. As the % content of the soft phase increased, the coercivity of the alloy decreased and remanence increased (Table 3). The remanence increases almost linearly with w, in agreement with experimental results [10,16], due to the higher magnetic moment of the soft phase.

Table 3: The effect of the % content of the soft phase on H_c

w*100%	1	10	20	30	40	50	60
$(\Delta H_c)\%$	-	0.48	0.49	0.49	1.98	2.02	2.06
$(\Delta M_r)\%$	-	3.3	3.5	3.6	3.7	3.8	3.9

The results obtained so far are suggesting that the proposed model can reproduce the hysteresis behaviour of inhomogeneous magnets. Future work involves the substitution of, the only one available for now, S-W-based $\Gamma(H_+, H_-)$ by other switching operators. This is dictated by the fact that the magnetization rotation in this type of magnets is not coherent. The use of the S-W astroid might be the reason why irreversible processes begin to manifest themselves at fields not lower than $0.6H_c$. The work presented in the first part of this paper will be the basis for designing a new appropriate switching mechanism. Second, an interactions distribution $\rho_3(H_i)$, other than a Gaussian, might be necessary. It has been mentioned already that stray fields become more prominent as the applied field, decreasing from H_{sat}, becomes negative. This suggests that the interactions distribution is not symmetrical around the axis of coercivities on the Preisach plane. Finally, an alternative approach is to use the model for irreversible processes only and then add the reversible component based on measurements of $x_{rev}(H)$ and $x_{irr}(H)$ [18].

6. CONCLUDING REMARKS

The comparison of existing analytical solutions for the nucleation field of a soft spherical inclusion inside a hard magnetic axis contributes to our knowledge of the magnetization process in inhomogeneous magnets. The results are incorporated in the design of a new model which is a first attempt to use Preisach -type models for inhomogeneous magnets. The model has successfully reproduced the hysteresis behavior of such alloys and the identification parameters have been related to microscopic and macroscopic material properties.

References

1. Kronmüller, H., "Theory of nucleation fields in inhomogeneous ferromagnets", *Phys. Stat. Sol. (b)*, 144, p.385 (1987).

2. Skomski, R., "Aligned two-phase magnets: Permanent magnetism of the future? (invited)", *J. Appl. Phys.* 76 (10), p.7059 (1994).

3. Skomski, R. and Coey, J.M.D., "Giant energy product in nanostructured two-phase magnets", *Physical Review B*, 48(21), p.15812 (1993).

4. Fischer, R., and Kronmüller, H., Static computational micromagnetism of demagnetization processes in nanoscaled permanent magnets, Physical Review B, 54(10), p.7284 (1996).

5. Schrefl, T., Fidler, J., Kronmüller, H., "Remanence and coercivity in isotropic nanocrystalline permanent magnets", *Physical Review B,* 49(9), p.6100 (1994).

6. Fredkin, D.R. and Koehler, T.R., Ab initio micromagnetic calculations for particles (invited), J. Appl. Phys., 67(9), p.5544 (1990).

7. Charap, S.H. and Ktena, A., "Vector Preisach modeling (invited)", *J.Appl.Phys.*, 73(10), p.5818 (1993).

8. Ktena, A. and Charap, S.H., "Vector Preisach Modeling and Recording Applications", *IEEE Transactions on Magnetics*, 29(6), p.3661 (1993).

9. Kirchmayr, H.R., "Permanent magnets and hard magnetic materials (invited)", J.Phys. D: App. Phys., 29, pp.1763-2778 (1996).

10. Bauer, J., Seeger,M., Zern, A. and Kronmüller, H., "Nanocrystalline FeNdB permanent magnets with enhanced remanence", J. Appl. Phys. 80 (3), p.1667 (1996).

11. Kou, X.C., Qiang, W.J., Kronmüller, H., and Schulz, L., "Coercivity of Sm-Fe-N ferromagnets produced by the mechanical alloying technique", *Journal of Applied Physics*, v.74, n.11, p.6791 (1993).

12. Kou, X.C., *et. al.*, "Magnetization reversal process of Zn-bonded anisotropic Sm-Fe-N permanent magnets", *Physical Review B*, 51(22), p.16025 (1995).

13. Ktena, A., Fotiadis, D.I. and Massalas, C.V., "Comparison of nucleation models for inhomogeneous ferromagnetic materials", Proceedings of the 5th National Congress on Mechanics, vol.2, pp.790-801 (1998).

14. Wiesen, K., and Charap, S.H., A better scalar preisach algorithm, IEEE Transactions on Magnetics, v.24, n.6, p.2491, 1988.

15. E.H.Feutrill, P.G. McCormick and R. Street, "Magnetization behavior in exchange-coupled $Sm_2Fe_{14}Ga_3C_2/\alpha$-Fe", J.Phys.D: Appl. Phys. 29, pp. 2320-2326 (1996).

16. H. Kronmüller, R. Fischer, M. Seeger and A. Zern, "Micromagnetism and microstructure of hard magnetic materials", J. Phys. D: Appl. Phys. 29, pp. 2274-2283 (1996).

17. J. van Lier, M. Seeger, H. Kronmüller, "Magnetic and microstructural properties of melt-spun FeGaSmC permanent magnets", Journal of Magnetism and Magnetic Materials, 167, pp.43-46 (1997).

18. Cammarano, R., McCormick, P.G., and Street, R., "The interrelation of reversible and irreversible magnetization", *Journal of Phyics D: Applied Physics*, v. 29, p. 2327-2331 (1996).

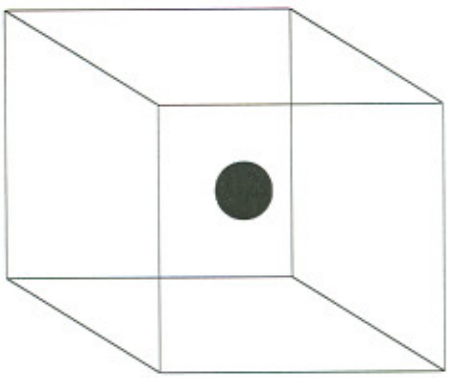

Fig. 1

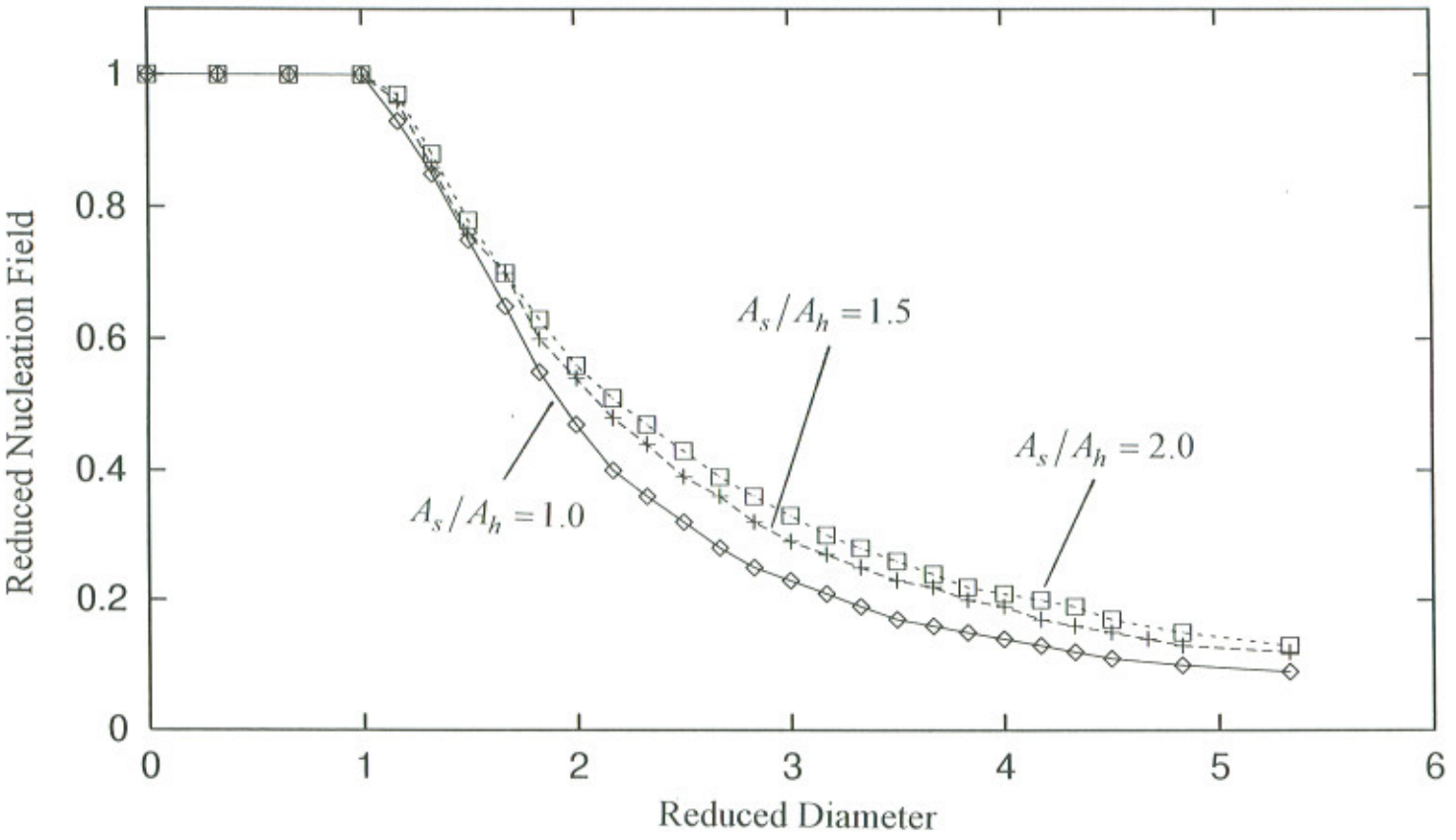
Reduced Nucleation Field
Reduced Diameter
$A_s/A_h = 1.0$
$A_s/A_h = 1.5$
$A_s/A_h = 2.0$
0
0.2
0.4
0.6
0.8
1
0
1
2
3
4
5
6

Fig. 2

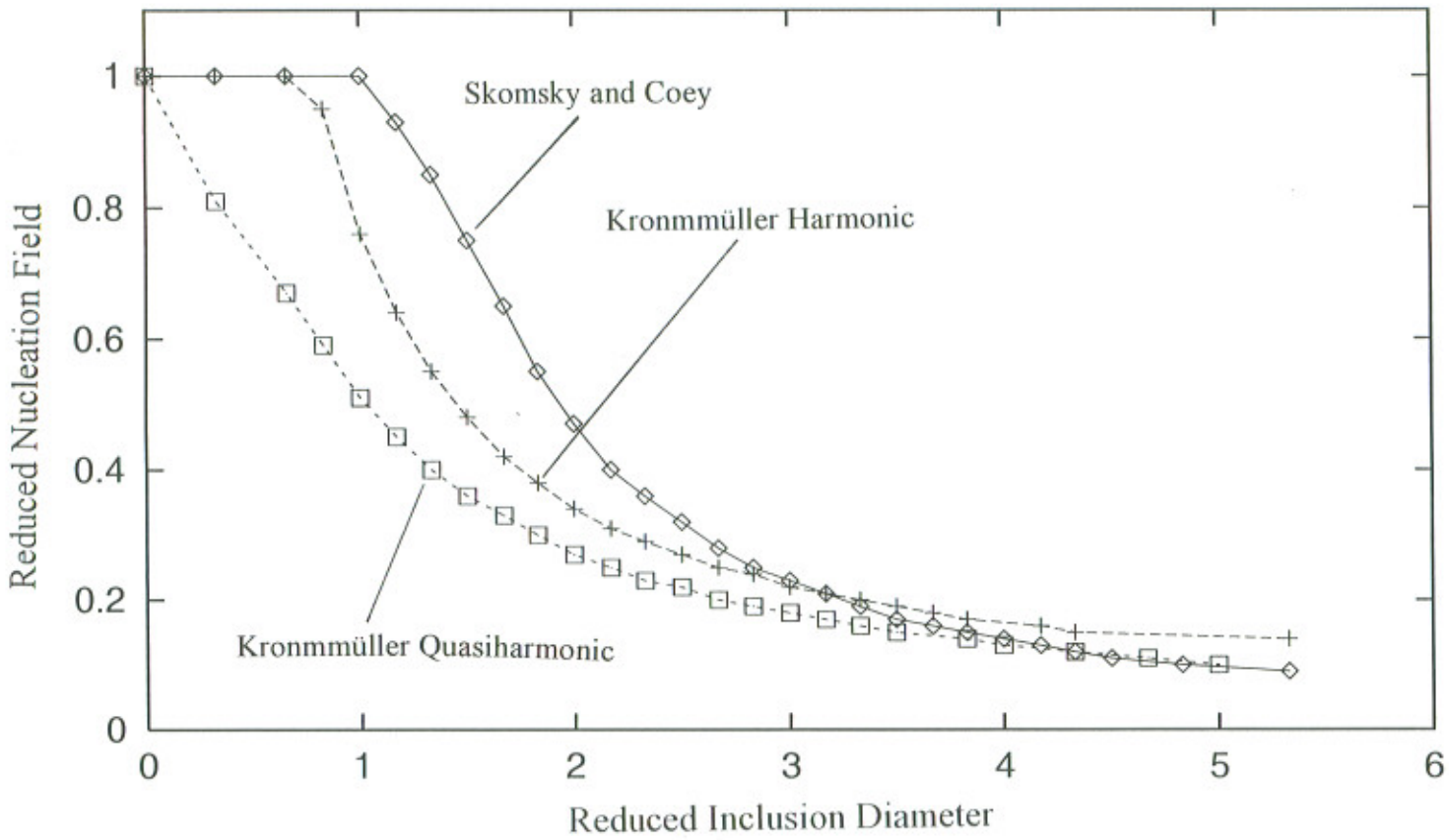
Skomsky and Coey
Kronmmüller Harmonic
Kronmmüller Quasiharmonic
Reduced Nucleation Field
Reduced Inclusion Diameter
0
0.2
0.4
0.6
0.8
1
0
1
2
3
4
5
6

Fig. 3

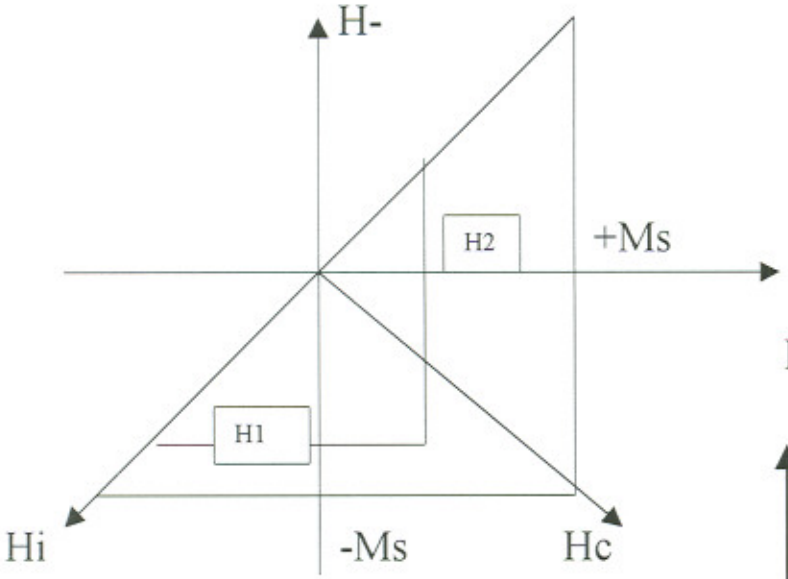

$\rho(H+, H-) = \rho(H_c, H_i)$
$= \rho(H_c)\ \rho(H_i)$

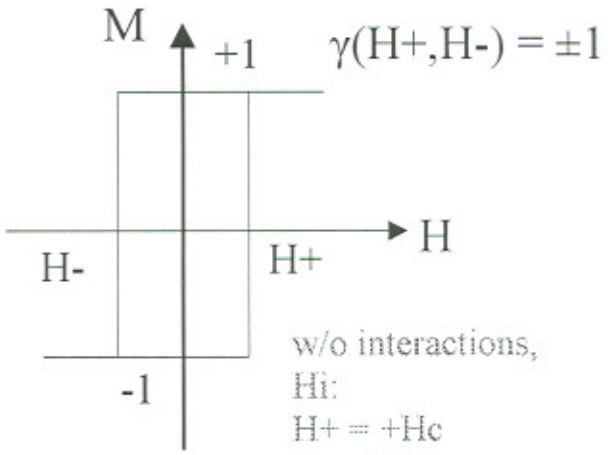

w/o interactions,
Hi:
H+ = +Hc
H- = -Hc

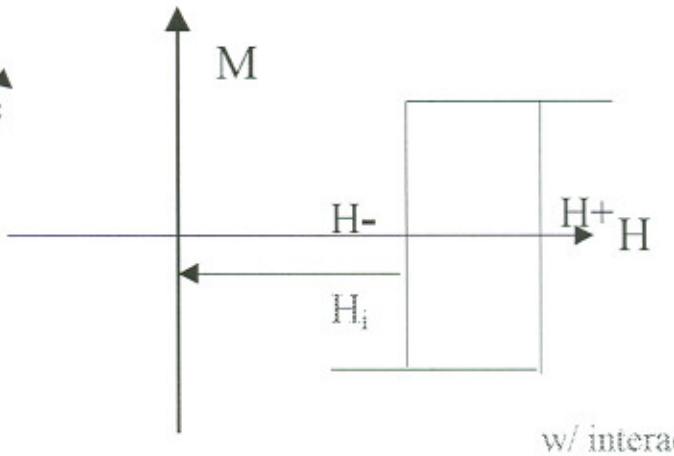

w/ interactions, Hi:
H+ = Hc - Hi
H- = -Hc + Hi

Fig. 4

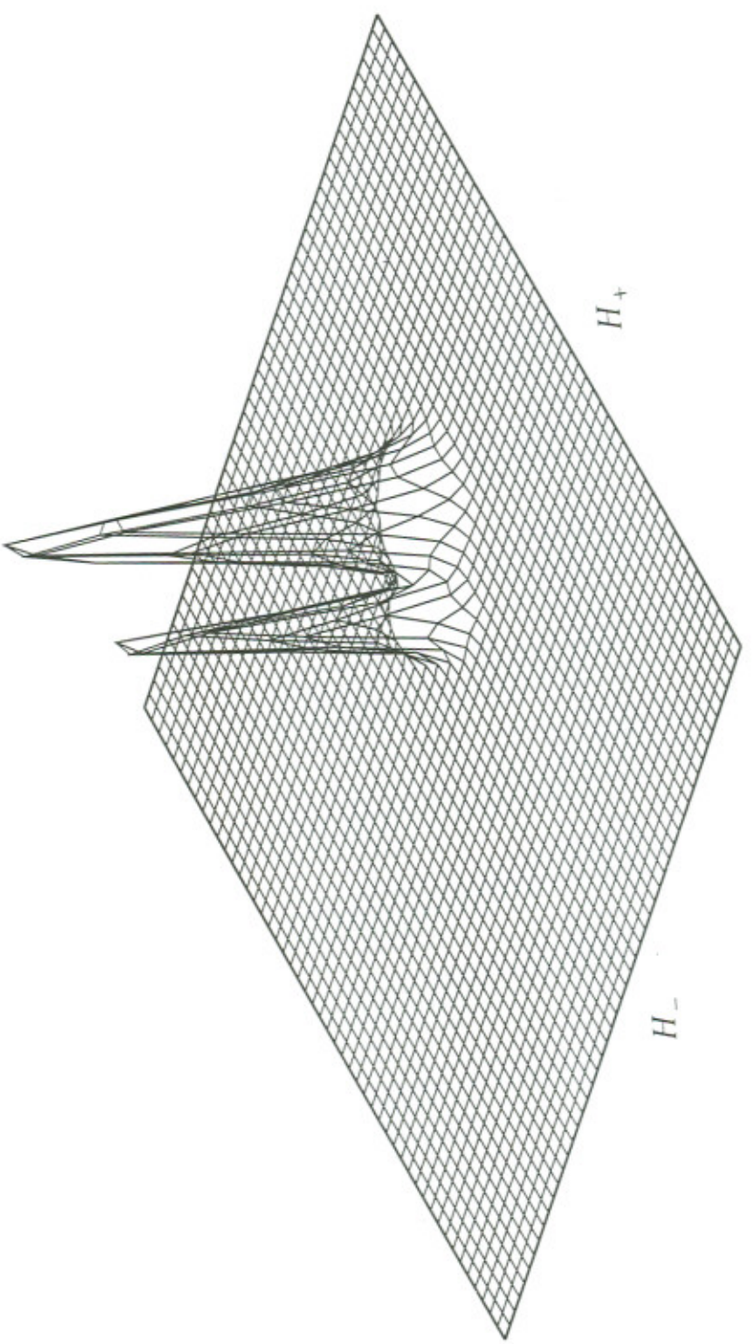

Fig. 5

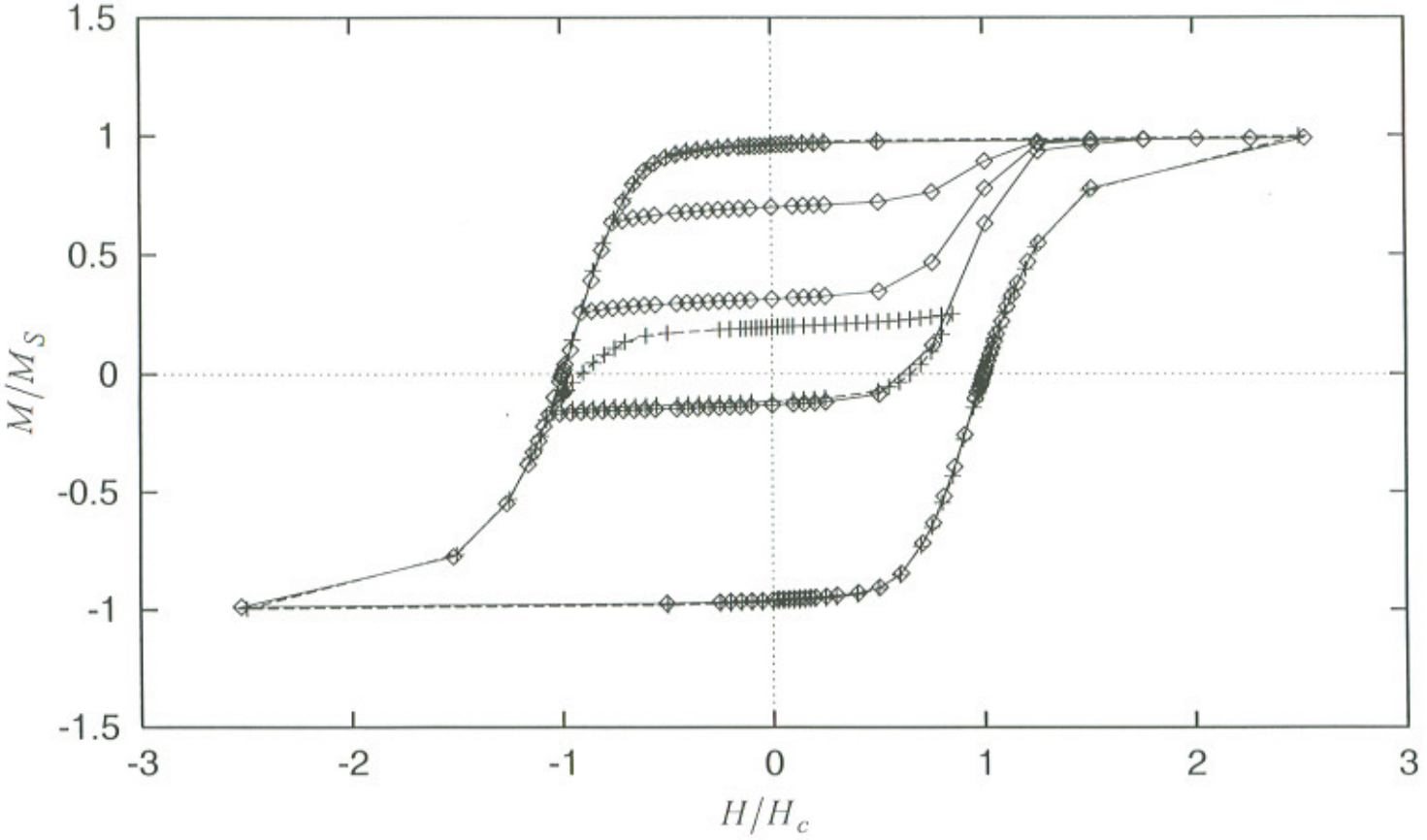

Fig. 6

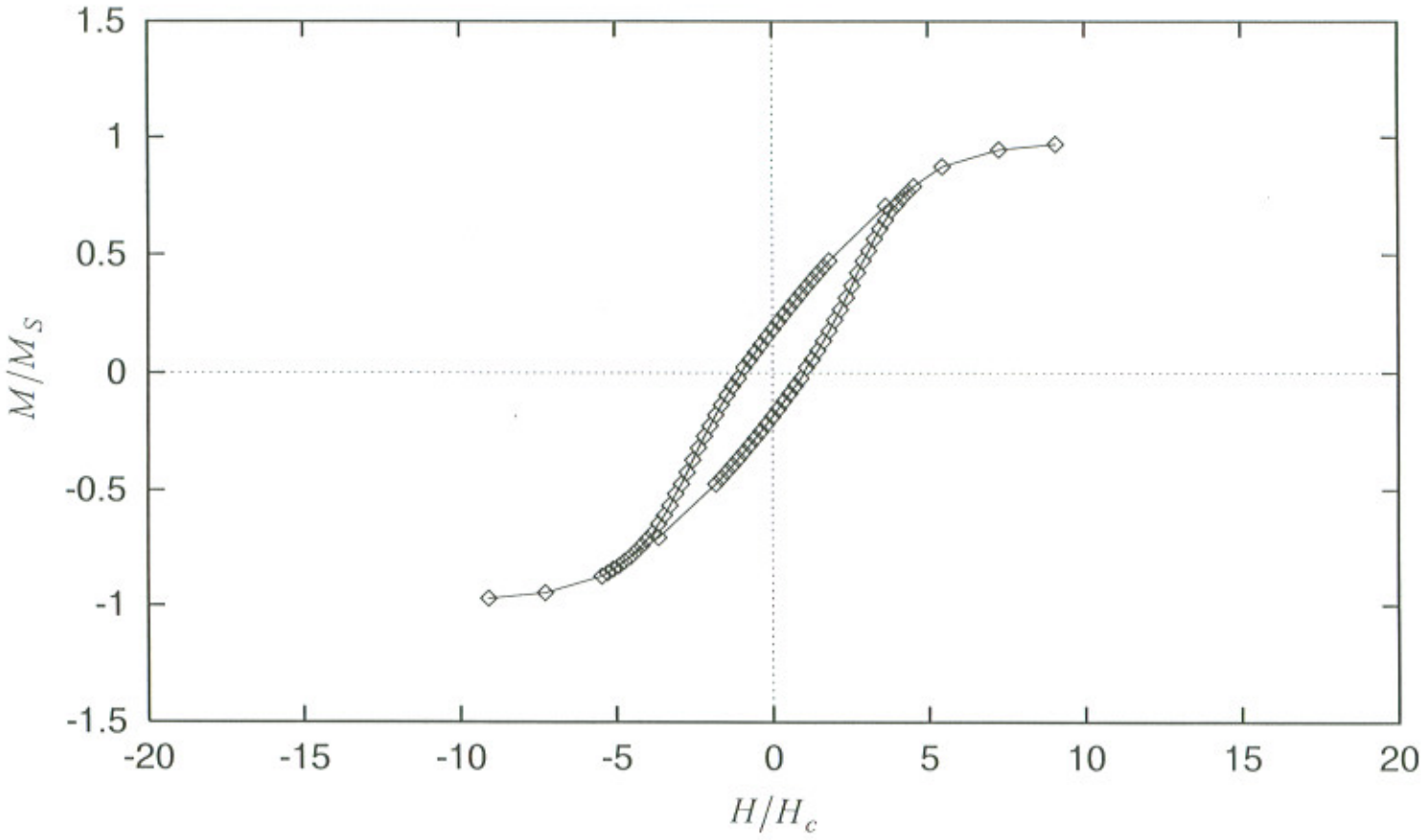

Fig. 7

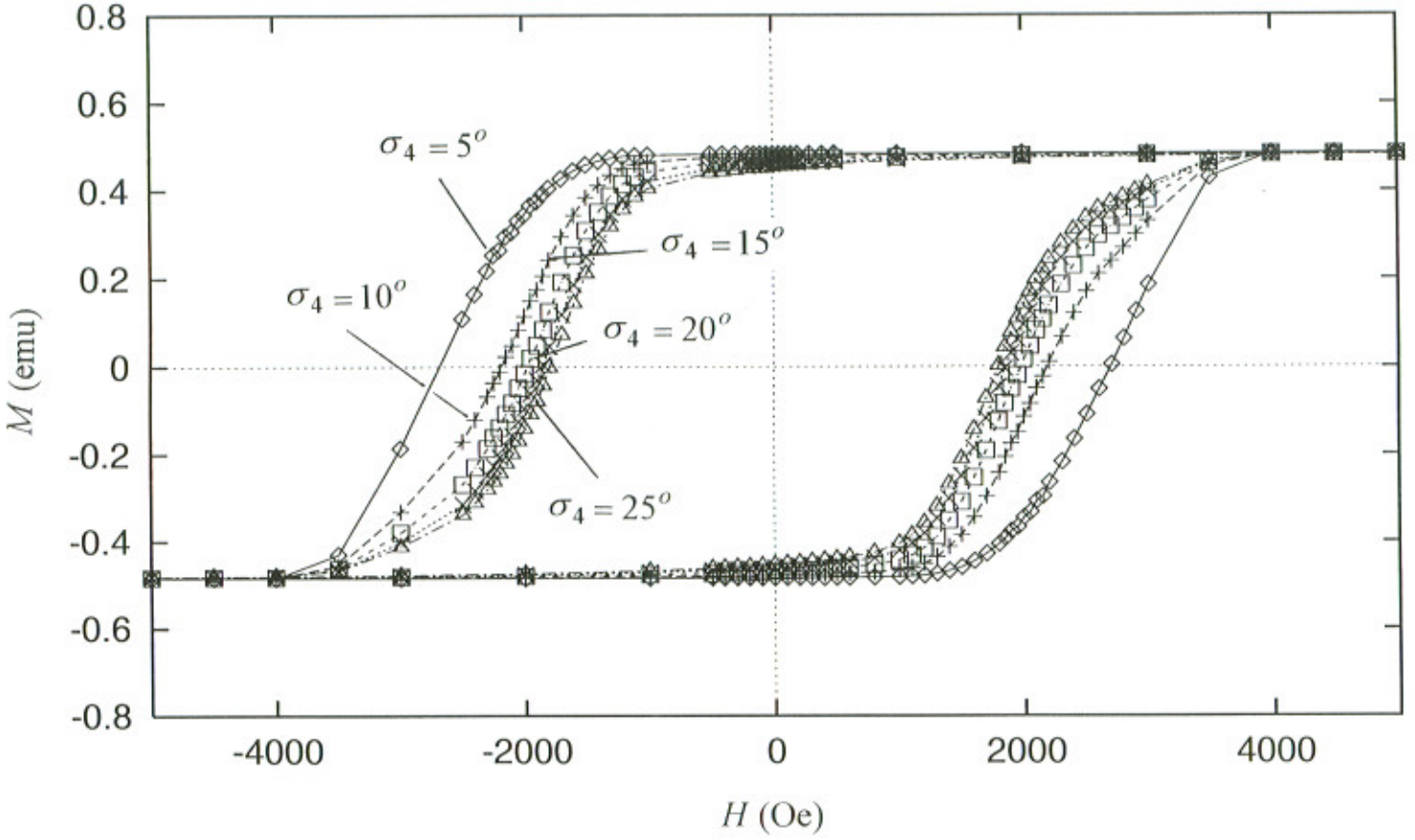
0.8
0.6
0.4
0.2
0
-0.2
-0.4
-0.6
-0.8
-4000
-2000
0
2000
4000
M (emu)
H (Oe)
$\sigma_4 = 5^o$
$\sigma_4 = 10^o$
$\sigma_4 = 15^o$
$\sigma_4 = 20^o$
$\sigma_4 = 25^o$

Fig. 8

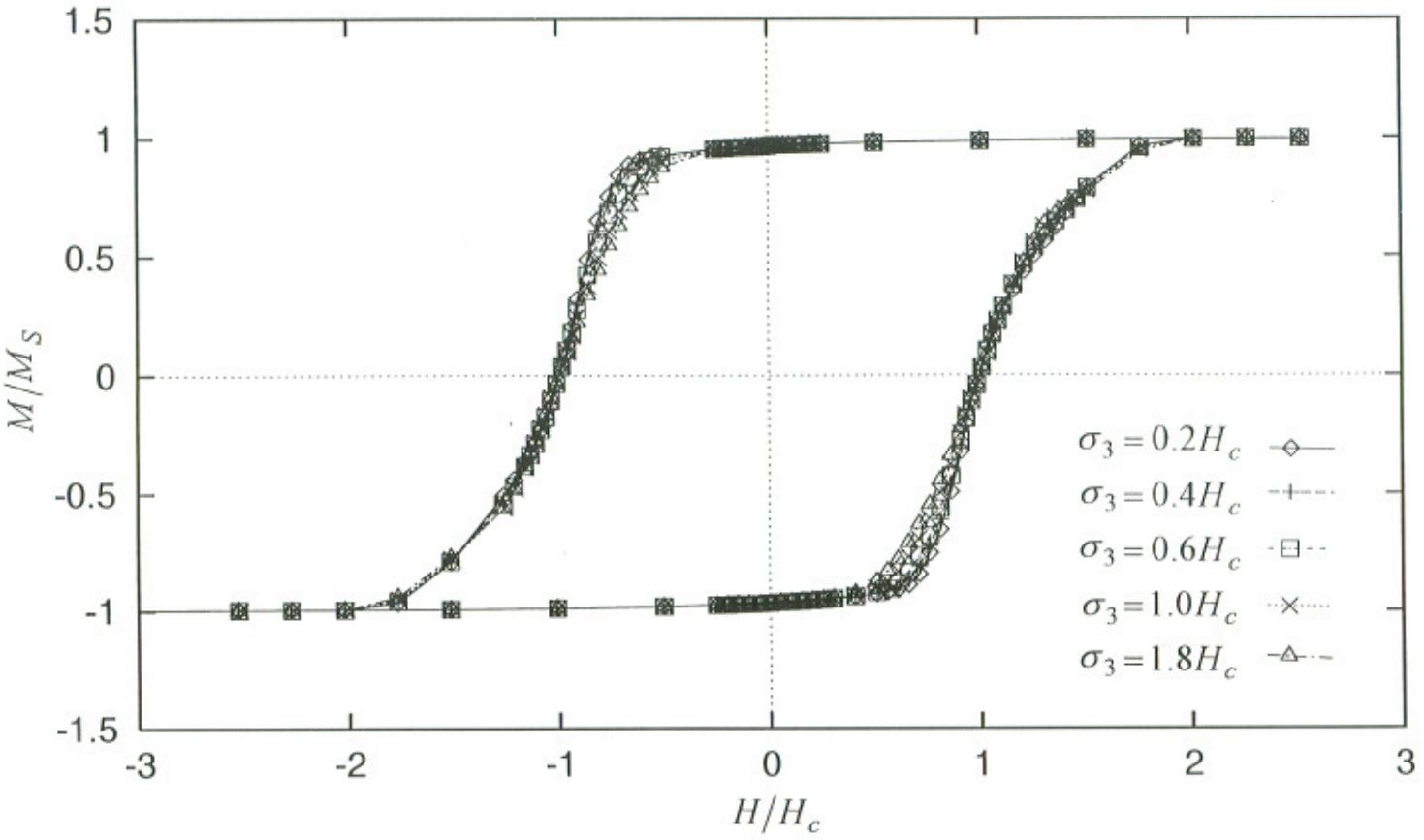
1.5
1
0.5
0
-0.5
-1
-1.5
-3
-2
-1
0
1
2
3
M/M_S
H/H_c
$\sigma_3 = 0.2H_c$
$\sigma_3 = 0.4H_c$
$\sigma_3 = 0.6H_c$
$\sigma_3 = 1.0H_c$
$\sigma_3 = 1.8H_c$

Fig. 9

Department of Computer Science
University of Ioannina

Technical Reports

1998

1-98: G.D. Akrivis, V.A. Dougalis, O.A. Karakashian, W.R. McKinney
"Numerical Approximation of Singular Solutions of the Damped. Nonlinear Schrödinger Equation"

2-98: P.A. Voltairas, D.I. Fotiadis, C.V. Massalas
"Micromagnetics of Thin Ferromagnetic Films under Mechanical Stress"

3-98: A. Likas, V.Th. Paschos
"A new solution representation for the travelling salesman problem"

4-98: D.G. Papageorgiou, I.N. Demetropoulos and I.E. Lagaris
"MERLIN - 3.0: A Multidimensional Optimization Environment"

5-98: D.G. Papageorgiou, I.N. Demetropoulos and I.E. Lagaris
"The Merlin Control Language for Strategic Optimization"

6-98: E. Pitoura and I. Fudos
"Address Forwarding in Hierarchical Location Directories for Mobile PCS Users"

7-98: I.E. Lagaris, A. Likas, D.G. Papageorgiou
"Neural Network Methods for Boundary Value Problems Defined in Arbitrarily Shaped Domains"

8-98: D.I. Fotiadis, G. Foutsitzi and Ch.V. Massalas
"Wave Propagation in Human Long Bones"

9-98: G. Samaras, E. Pitoura
"Computational Models for Wireless and Mobile Environments"

10-98: E. Pitoura
"Transaction-Based Coordination of Software Agents"

11-98: A. Charalambopoulos, D.I. Fotiadis and C.V. Massalas
"Biomechanics of the Human Cranial System"

12-98: A. Charalambopoulos, D.I. Fotiadis and C.V. Massalas
"Dynamic Response of the Human Head to an External Stimulus"

13-98: E. Pitoura
"Supporting Read-Only Transaction in Wireless Broadcasting"

14-98: S.D. Nikolopoulos
"On the Structure of A-free Graphs"

15-98: A. Ktenas, D.I. Fotiadis and C.V. Massalas
"Comparison of Nucleation Models for Inhomogeneous Ferromagnetic Materials"

16-98: A. Likas
"Multivalued Parallel Recombinative Reinforcement Learning: A Multivalued Genetic Algorithm"

17-98: A. Likas, A. Stafylopatis
"Training the Random Neural Network Using Quasi-Newton Methods"

18-98: D.I. Fotiadis, G. Foutsitzi and C.V. Massalas
"Wave Propagation Modeling in Human Long Bones"

19-98: P.A. Voltairas, D.I. Fotiadis and C.V. Massalas
"Effect of Magnetostriction on the Magnetization Reversal of a Fine Particle in a Solid Non-Magnetic Matrix"

20-98: E. Pitoura and G. Samaras
"Locating Objects in Mobile Computing"

21-98: E. Pitoura
"Scalable Invalidation-Based Processing of Queries in Broadcast Push Delivery"

22-98: A. Likas
"Probability Density Estimation Using Multilayer Perceptrons"

23-98: K.N. Malizos, M.S. Siafakas, D.I. Fotiadis, P.N. Soucacos
"Semiautomated Volumetric Description of Osteonecroses"

24-98: N. Vlassis, A. Likas
"The Kurtosis-EM algorithm for Gaussian mixture modelling"

25-98: P. Rondogiannis
"Stratified Negation in Temporal Logic Programming and the Cycle Sum Test"

26-98: E. Pitoura, P. Chrysanthis
"Scalable Processing of Read-Only Transactions in Broadcast Push"

27-98: D. Barelos, E. Pitoura, G. Samaras
"Mobile Agent Procedures: Metacomputing in Java"

28-98: A. Likas
"A Reinforcement Learning Approach to On-line Clustering"

29-98: P.A. Voltairas, D.I. Fotiadis and C.V. Massalas
"The Role of Material Parameters and Mechanical Stresses on Magnetic and Magnetostrictive Hysteresis"

Department of Computer Science
University of Ioannina

Technical Reports

1999

1-99: V.V. Dimakopoulos
Single-Port Multinode Broadcasting

2-99: E. Pitoura, P.K. Chrysanthis
Exploiting Versions for Handling Updates in Broadcast Disks

3-99: P. Rondogianiis and M. Gergatsoulis
"The Branching-Time Transformation Technique for Chain Datalog Programs"

4-99: P.A. Voltairas, D.I. Fotiadis and C.V. Massalas
"Nonuniform Magnetization Reversal In Stressed Thin Ferromagnetic Films"

5-99: S.D. Nikolopoulos
"Coloring Permutation Graphs in Parallel"

6-99: A.P. Liavas
"Least-squares channel equalization performance versus equalization delay"

7-99: I. Fudos and L. Palios
"An Efficient Shape-based Approach to Image Retrieval"

8-99: D.I. Fotiadis, G. Foutsitzi and C.V. Massalas
"Wave Propagation in Human Long Bones of Arbitrary Cross Section"

9-99: V.S. Kodogiannis, E.M. Anagnostakis
"Soft Computing Based Techniques for Short-term Load Forecasting"

10-99: V.S. Kodogiannis
"A Study on Attitude Controle Schemes Based on Neural Network Structures"

11-99: V.S. Kodogiannis
"A Neural Network-Based Detection Thresholding Scheme for Active Sonar Signal Tracking"

12-99: V.S. Kodogiannis
"Compurison of Advanced Learning Algorithms for Short-term Load Forecasting"

13-99: V.S. Kodogiannis
"Development of a Breast Cancer Diagnostic System Via a Fuzzy-genetic Scheme"

14-99: P. Rondogiannis
"Adding Multidimensionality to Procedural Programming Languages"

15-99: P.A. Voltairas, D.I. Fotiadis and C.V. Massalas
"Magnetization Curling in an Elastic Sphere
(An pper Bound to the Nucleation Field)

16-99: A. Charalambopoulos, G. Dassios, D.I. Fotiadis and C.V. Massalas
"Scattering of a Point Generated Field by a Multilayered Spheroid"

17-99: A. Ktena, D.I. Fotiadis and C.V. Massalas
"A New 2-D Model for Inhomogeneous Permanent Magnets"